Effects of Valency on Thermodynamic Parameters of Specific Membrane Interactions†

Bruce P. Babbitt and Leaf Huang*
Department of Biochemistry, University of Tennessee, Knoxville, Tennessee 37996-0840
Received June 26, 1984; Revised Manuscript Received November 28, 1984

ABSTRACT: We have measured the equilibrium binding of dioleoylphosphatidylcholine vesicles (800-Å diameter) containing various densities of incorporated palmitoyl-α-bungarotoxin (PBGT) to acetylcholine receptor (AchR) enriched microsac membranes. We have previously shown that these PBGT vesicles bind specifically to the microsacs mediated by direct interactions with the AchRs [Grant, S. W., Babbitt, B. P., West, L. K., & Huang, L. (1982) *Biochemistry 21*, 1274–1279]. The percent binding of liposomal lipid and associated PBGT to excess AchR sites, as well as the inhibition of binding by pretreatment of microsacs with excess α-bungarotoxin (αBGT), was strongly dependent upon the protein/lipid molar ratio of the vesicles. In addition, there existed a threshold level of approximately six PBGT molecules per vesicle at which the binding increased dramatically. The apparent association constant, K_A^{app}, for lipid vesicle–microsac membrane binding increased approximately 4800-fold (from 3.95×10^4 to 1.90×10^8 M^{-1}) due to an increase of 20-fold in the vesicle-associated PBGT surface density. Direct competition for binding to microsac membranes between vesicles with different PBGT/lipid molar ratios indicated that multivalent binders could easily replace binders of lower valency when receptor sites were limited. Measurement of the temperature dependence of the K_A^{app} indicated that weak (low valency) and medium strength (intermediate valency) PBGT vesicle binders bound to microsacs in a fashion similar to the binding of αBGT and PBGT to detergent-solubilized AchRs. Strong PBGT vesicle binders (high valency) appear to bind by a somewhat different mechanism. All results are discussed in terms of the effects of ligand (PBGT) valency on the binding strength of vesicles to microsac membranes.

Vital cellular processes such as proliferation, motility, morphology, and differentiation are thought to be controlled in part by extracellular signals received at the cell surface (Ruter, 1978; Subtelny & Wessels, 1980). An important example of such a control process is the modification of cell behavior by direct cell–cell contact. Presumably, a specific cell surface receptor can bind stereospecifically to a mutually complementary receptor on an apposing cell surface followed by translation of the binding event into a cellular response (Frazier & Glaser, 1979). Although there are many (somewhat) well-documented systems in which the presence of specific molecules (CAM, SAM, lectins, antibodies, etc.) are required (or are inferred from the specificity of the interaction) in order for cell–cell or cell–substratum adhesion to occur (Frazier et al., 1982; Edelman, 1983; Springer & Barondes, 1982), the molecular mechanisms for cell–cell recognition have been elusive because of their complexity. Pioneer theoretical works describing such interactions have recently been reported by Bell et al. (1984) in which they undertake a thermodynamic approach to the modeling of cell adhesion, resulting in a number of explicit but unsubstantiated predictions. In order to simplify the experimental design for the basic physicochemical study of cell–cell recognition, we have previously developed a model system for the study of specific membrane–membrane binding mediated by specific membrane-associated ligands and receptors. We chose to incorporate the snake venom toxin α-bungarotoxin onto the surface of lipid vesicles [achieved by acylation of the toxin generating palmitoyl-α-bungarotoxin (PBGT)[1] followed by spontaneous insertion of the protein into preformed lipid vesicles] and to study the thermodynamics of the PBGT vesicle interaction with microsac membranes highly enriched with nicotinic acetylcholine receptors (AchRs). In a recent publication (Grant et al., 1982), we have described the initial development of such a model system and have further shown that PBGT vesicles bind to microsac membranes via specific interactions with AchRs as evidenced by their ability to quantitatively inhibit AchR-enriched microsac ion channel activity. We have also characterized the vesicle-associated PBGT from the standpoint of the PBGT mobility on the vesicle surface (Babbitt et al., 1984) and the orientation of PBGT when anchored to the vesicle bilayer by the acyl chain (Babbitt & Huang, 1985). In this report, we present a detailed thermodynamic characterization of the binding of PBGT vesicles to AchR-enriched microsac membranes as mediated by specific toxin–receptor interactions. Special attention is paid to the role of valency in determination of the equilibrium binding parameters.

Materials and Methods

Materials. Purification and iodination of αBGT, synthesis, purification, and radiolabeling of PBGT, and preparation of acetylcholine receptor enriched microsac membrane vesicles were all performed as previously described (Grant et al., 1982).

PBGT Binding to Detergent-Solubilized Acetylcholine Receptor. The binding of PBGT and αBGT to Triton X-100 solubilized AchR from *Torpedo californica* was assayed by using Whatman DE-81 filters as previously described (Grant et al., 1982). PBGT affinity for AchR was found to be approximately 20-fold lower than that for the native toxin, and

† This work was supported by National Institutes of Health Grant GM 31724 and a Research Career Development Award to L.H. (CA 00718).

[1] Abbreviations: αBGT, α-bungarotoxin; PBGT, palmitoyl-α-bungarotoxin; DOPC, dioleoylphosphatidylcholine; PBS, phosphate-buffered saline (137 mM NaCl, 2.7 mM KCl, 1.5 mM KH_2PO_4, and 1.0 mM Na_2HPO_4, pH 7.4); AchR, acetylcholine receptor; SUV, small unilamellar vesicles; EGTA, [ethylenebis(oxyethylenenitrilo)]tetraacetic acid; SDS, sodium dodecyl sulfate.

0006-2960/85/0424-2186$01.50/0

PBGT bound specifically and as a homogeneous species to the same class of receptor as the native toxin as previously reported (Babbitt & Huang, 1985).

Analytical Methods. Protein (αBGT) was determined spectrophotometrically by using an absorption coefficient, $A^{1\%}_{280}$, of 12.0 (Chen et al., 1982). ^{125}I cpm were directly counted by using a Beckman Biogamma II counter. ^{3}H cpm were counted in a Beckman LS-230 liquid scintillation counter using a Triton X-100/toluene cocktail. All results were corrected for channel crossover if more than one isotope was employed.

Vesicle Formation and Incorporation of PBGT into Lipid Vesicles. The detergent dialysis method of Enoch & Strittmatter (1979) was used with modifications. Dioleoylphosphatidylcholine (DOPC) at 14 mg/mL with a trace amount of hexadecyl[^{3}H]cholestanyl ether (a nonexchangeable lipid marker) (Pool et al., 1982) at a final specific activity of 1.25×10^4 cpm/nmol was suspended in phosphate-buffered saline containing 0.02% sodium azide and 2.5 mM EGTA ($PBS/N_3/EGTA$) at pH 8.0. The suspension was sonicated for 20 min at 4 °C in a bath sonicator (Laboratory Supplies Co., Hicksville, NY) in order to generate SUV. A 4.9% solution of deoxycholate in $PBS/N_3/EGTA$ was added to the SUV to yield a mixed micellar solution of 6 mg/mL in lipid and 0.82% in detergent. The resultant clear solution was next dialyzed at room temperature in a Spectrapor-2 dialysis membrane against 8000 volumes of $PBS/N_3/EGTA$ at pH 8.0 for 48 h, followed by dialysis against 4000 volumes of $PBS/N_3/EGTA$ at pH 7.4 for 24 h. All samples became turbid approximately 8–10 h after initiation of dialysis. Following the dialysis at pH 7.4, all samples were centrifuged at 3000*g* for 20 min in order to pellet residual aggregated detergent. In order to remove SUV and any residual soluble detergent from the vesicle suspension, the supernatant was fractionated through a Bio-Gel A50m column, and vesicles eluting in the void volume were pooled and stored under N_2 at 4 °C as our DOPC "preformed" vesicle stock. For incorporation of PBGT into the vesicles, 1-mL aliquots of DOPC vesicles adjusted to 6 mg/mL were mixed with 500-μL suspensions containing various amounts of ^{125}I-PBGT at a specific activity of 1.08×10^6 cpm/nmol in $PBS/N_3/EGTA$, pH 7.4, and incubated overnight at 37 °C to allow for equilibrium association of the acylated protein with the lipid bilayer (Babbitt et al., 1984). The PBGT vesicles were then rechromatographed over a Bio-Gel A50m column to remove unincorporated PBGT and small particles generated by the incorporation procedure. Void volume fractions were pooled and stored as our PBGT vesicle stocks under N_2 at 4 °C until further use.

Characterization of PBGT Vesicles. (*A*) *Sucrose Density Gradients.* Each gradient consisted of a 4.5-mL 5–20% linear sucrose gradient with a 0.5-mL 65% sucrose cushion. A 10–20-μL sample of the PBGT vesicles (approximately 300 μg of lipid) was layered on top of the gradient and centrifuged at 190000*g* in an SW 50.1 Beckman swinging-bucket rotor for 24 h at 4 °C. Following centrifugation, 100-μL fractions were collected from the bottom of the gradient by using a Pharmacia peristaltic pump. ^{125}I cpm were counted directly, and 20-μL aliquots were counted for ^{3}H cpm in order to monitor the migration of protein and lipid, respectively.

(*B*) *Column Chromatography.* In order to determine the size distribution of the PBGT vesicles, especially to assay for the presence of small vesicles, 20-μL samples of each PBGT vesicle preparation were fractionated through 5-mL Bio-Gel A50m columns, and 150-μL fractions were collected and counted for ^{125}I and ^{3}H cpm. All vesicle preparations, regardless of the amount of associated PBGT, quantitatively voided the column, indicating that incorporation of relatively large amounts of protein did not solubilize or dramatically decrease vesicle size. In addition, PBGT in vesicle suspensions of protein/lipid molar ratios less than 2.5×10^{-3} quantitatively voided the column with the lipid while vesicle suspensions of molar ratios greater than 2.5×10^{-3} showed two peaks of PBGT: one peak voided the column with the lipid, and a second broad peak remained well included and was identified as non-vesicle-associated, aggregated PBGT.

(*C*) *Electron Microscopy.* A 5-μL sample of PBGT vesicles adjusted to 6 mg/mL in lipid was placed on carbon-stabilized, formvar-coated copper grids which were glow discharged immediately before use. Vesicles were negatively stained with 1% potassium phosphotungstate at pH 7.5. They were viewed at various magnifications with a Hitachi H-600 microscope in the transmission mode at 75 kV. Alternatively, vesicles were visualized by utilizing the electron-scattering and secondary-imaging modes of the microscope. To determine the size distribution of the vesicles, a histogram was obtained by measuring more than 100 vesicles from each vesicle preparation. PBGT vesicles were found to be quite homogeneous with an average diameter of 800 ± 80 Å. A small population (less than 15% of the total lipid) of small vesicles was present, and the incorporation of PBGT at protein/lipid molar ratios between 0 and 2.5×10^{-3} appeared to have no perceptible effect on the size of the vesicles. The key factor in determining vesicle size appears to be the deoxycholate/lipid molar ratio in the initial detergent dialysis mixture. For example, the average diameter of the vesicle becomes 600 Å if the detergent/lipid molar ratio used is decreased from 2.8 to 1.4.

Binding of PBGT Vesicles to Microsac Membranes Enriched with AchR. The equilibrium binding of PBGT vesicles to microsac membranes enriched with AchR was studied as a function of the protein/lipid molar ratio of the vesicle population. Ten picomoles of vesicle-associated PBGT in 30 μL of $PBS/N_3/EGTA$, pH 7.4, was added to 51.2 μg (total protein) of AchR-enriched vesicles in 60 μL of the same buffer.

Following incubation for 5 h at room temperature, 30-μL aliquots of the PBGT vesicle–microsac suspension were layered over a 150-μL 5% sucrose solution in a 5 × 20 mm polyallomer tube and spun at 165000*g* (generated at 30 psi air pressure) for 15 min in a 30° fixed-angle rotor employing a Beckman Airfuge. Following centrifugation, the samples in the polyallomer tubes were frozen at −70 °C for at least 30 min, then sliced with a razor blade into a top (120 μL, supernatant) and bottom (60 μL, pellet) portion, and counted directly for ^{125}I cpm (protein). Thereafter, 380 and 440 μL of 10% SDS in distilled water was added to the supernatant and pellet fractions, respectively, and incubated overnight at 37 °C to dissolve the pellets. ^{3}H cpm (lipid) was then counted as previously described. Triplet samples were assayed for percent binding (pellet cpm/total cpm). All PBGT vesicle preparations were centrifuged alone under the aforementioned conditions to "preselect" for those vesicles that by themselves float on top of 5% sucrose, while microsacs were likewise preselected for their ability to pellet under the same centrifugation conditions, yielding a final preparation containing approximately 0.32 nmol of toxin binding sites/mg of protein.

In order to measure the binding affinity of PBGT vesicles for AchR-enriched microsac membranes as a function of the protein/lipid molar ratio of the vesicle population, PBGT vesicles were added at various concentrations in 30 μL of $PBS/N_3/EGTA$, pH 7.4, to 4 μg (total protein) of AchR-enriched microsacs in 60 μL of the same buffer. Following

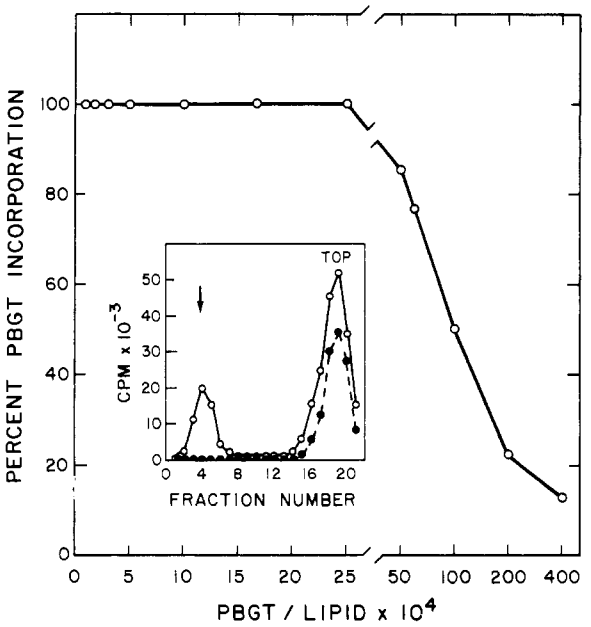

FIGURE 1: Dependence of PBGT incorporation efficiency upon the protein/lipid molar ratio of the PBGT–DOPC vesicle mixture. Inset: Sucrose density gradient centrifugation of a mixture of PBGT and DOPC vesicles (protein/lipid molar ratio of 6.0×10^{-3}) incubated at 37 °C for 24 h. The arrow denotes where free PBGT sedimented in a control gradient. (●) ^{3}H cpm (lipid); (○) ^{125}I-PBGT.

incubation for 5 h at room temperature, 30-μL aliquots of the PBGT vesicle–microsac suspension were assayed for binding in triplicate as mentioned previously. The data were analyzed by Scatchard plots (Scatchard, 1949), and the apparent association constant, K_A, was obtained from the slopes.

Competition Experiments. Either 6.8 nmol (17 pmol of vesicle-associated PBGT) of radiolabeled PBGT vesicle lipid at a protein/lipid molar ratio of 2.5×10^{-3} or 215 nmol (43 pmol of vesicle-associated PBGT) of radiolabeled PBGT vesicle lipid at a protein/lipid molar ratio of 2.0×10^{-4}, in 10 μL of PBS/N_3/EGTA, pH 7.4, was mixed with increasing concentrations of unlabeled competitor in 20 μL of PBS/N_3/EGTA, pH 7.4, and incubated with 2 or 8 μg (total protein), respectively, of AchR-enriched microsacs in 60 μL of the same buffer. Following a 5-h incubation at room temperature, 30-μL aliquots of the suspension were assayed in triplicate for binding as described previously.

RESULTS

Sucrose Density Gradient Analysis of PBGT Vesicles. The physical association of PBGT with the liposomal lipids was directly monitored by analytical sucrose density gradient ultracentrifugation. As shown in Figure 1, the incorporation efficiency is dependent upon the protein/lipid molar ratio and maintains a level of 100% until a molar ratio of 2.5×10^{-3} is exceeded. Assuming a vesicle average diameter of 800 Å (see electron microscopy results below) and approximately 60 000 phospholipid molecules per vesicle (Enoch & Strittmatter, 1979), it appears that we are able to incorporate approximately 150 PBGT molecules at 100% efficiency onto the surface of the vesicle. Using proteolysis as a probe of protein accessibility on the vesicle surface, we have previously shown that PBGT vesicles generated in a similar manner contain essentially 100% of the protein on the outer monolayer (Babbitt et al., 1984). The decrease in incorporation efficiency at protein/lipid molar ratios greater than 2.5×10^{-3} is probably due to steric hindrance rather than some facet of the incorporation protocol since a similar limit to the number of PBGT molecules at the outer monolayer was also seen when PBGT was incorporated into lipid vesicles by an entirely different technique, namely, detergent dialysis (data not shown). In the inset of Figure 1 is shown a typical sucrose density gradient sedimentation profile in which PBGT self-aggregated in aqueous buffer sediments toward the bottom of the gradient while PBGT incubated with lipid vesicles cosediments with the lipid on top of the gradient; vesicles by themselves also float on top of the gradient.

As a consequence of these data, we decided to prepare PBGT vesicles at protein/lipid molar ratios between 0 and 2.5×10^{-3} for all binding studies. Although it is possible to incorporate more PBGT per vesicle (up to a protein/lipid molar ratio of 4.0×10^{-3}; see Figure 1), we wanted to avoid the potential problem of ligand (PBGT) crowding on the vesicle surface in order to allow a more straightforward interpretation of the vesicle–microsac binding data, as well as to avoid the need for preparative sucrose density gradients to fractionate aggregated PBGT from vesicle-associated PBGT. Our previous measurements of rotational correlation times of vesicle-associated PBGT and the effect of incorporated PBGT on the thermotropic behavior of the vesicle lipid (Babbitt et al., 1984) had already indicated to us that the PBGT (ligand) was still fully dispersed and rotationally mobile on the vesicle surface at protein/lipid molar ratios as high as 5.0×10^{-3}. Our results indicate that incubation of an aqueous suspension of acylated toxin with vesicles preformed by the detergent dialysis method yields a quantitative and stable incorporation of PBGT into the outer leaflet of the lipid vesicles at protein/lipid molar ratios $\leq 2.5 \times 10^{-3}$.

Binding of PBGT Vesicles to Microsac Membranes Enriched with AchR. The equilibrium binding of PBGT vesicles to AchR-enriched microsac membranes was performed with the AchR sites in great excess of the amount of PBGT vesicle offered (at least 50-fold excess) so as to allow all binding-competent vesicles in a given population to bind without limitation due to site availability or vesicle–vesicle crowding on the microsac surface. Maximal vesicle binding occurred within 45–60 min for all vesicle preparations tested such that the percent PBGT and lipid binding was the same at 1 and 5 h of incubation. As shown in Figure 2, the percent binding of PBGT vesicles to microsacs was a sensitive function of the protein/lipid molar ratio of the vesicle population. Very little binding was detectable at protein/lipid molar ratios between 0 and 1.0×10^{-4} whereas PBGT vesicle binding above molar ratios of 1.0×10^{-4} increased significantly to a maximum of approximately 78% protein binding and 67% lipid binding at the highest protein/lipid molar ratio tested. This close correlation between lipid and protein percent binding is not unexpected since we did not directly measure the number of toxin–receptor complexes mediating the binding of vesicles to microsacs. Instead, we measured as "bound" all of the PBGT associated with vesicles that were bound to microsacs, even though not all of the PBGT molecules were involved in complexes with AchRs. Consequently, it is more informative to consider the effect of protein/lipid molar ratio on the percent binding of vesicles (lipid) to microsacs which is mediated by specific PBGT–AchR bridges. The close correlation between vesicle lipid and vesicle-associated PBGT binding also indicated that intact PBGT vesicles were binding to microsacs; i.e., PBGT was not pulled out of the vesicle upon interaction with microsac AchRs. The small difference in the lipid and protein percent binding is probably due to a small degree of PBGT vesicle heterogeneity. Therefore, as expected, the difference in percent lipid vs. percent PBGT binding decreased as the average protein/lipid molar ratio of the vesicle-associated

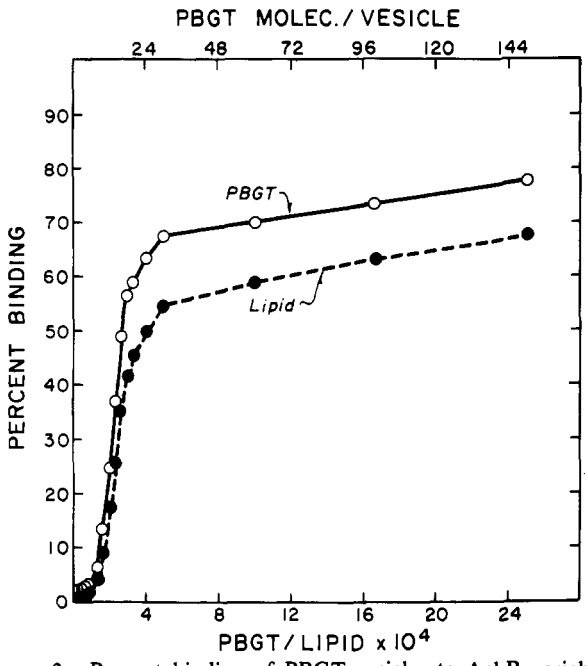

FIGURE 2: Percent binding of PBGT vesicles to AchR-enriched microsac membranes as a function of PBGT vesicle protein/lipid molar ratio.

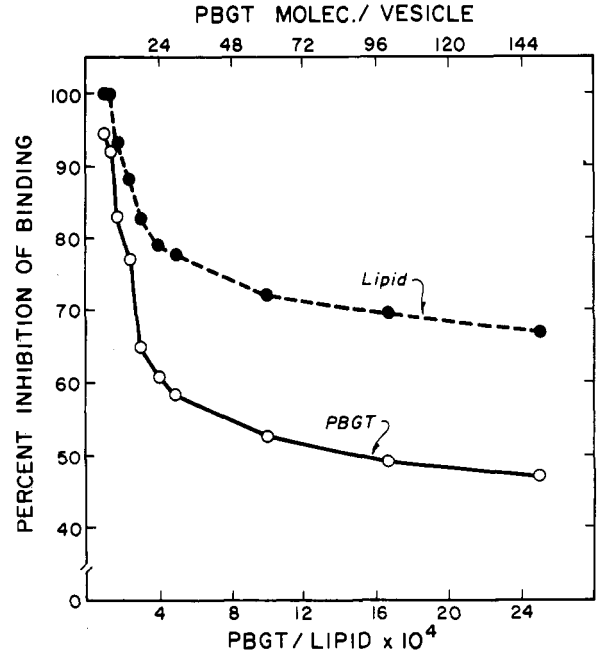

FIGURE 3: Percent inhibition of binding of PBGT vesicles to AchR-enriched microsac membranes pretreated with a 50-fold excess of αBGT as a function of PBGT vesicle protein/lipid molar ratio.

PBGT increased since fewer vesicles with little or no PBGT–vesicle were present in the population and unable to bind to microsacs. In separate control experiments, unlabeled lipid vesicles with no protein were added in appropriate amounts to each PBGT vesicle population in order to determine whether the low percent binding at the lowest protein/lipid molar ratios was due to inhibition of PBGT vesicles by bare vesicles. We found no change in the percent radiolabeled lipid or protein binding, indicating that bare vesicles did not inhibit PBGT vesicle binding to microsacs under conditions in which the AchR sites were in excess. Finally, it is interesting to note that there appears to be a threshold number of PBGT per vesicle, approximately 6, above which the vesicle binding increases significantly.

In Figure 3 are shown the results of an experiment in which a large excess of unlabeled αBGT in a 50-fold excess of AchR sites was incubated with the microsacs prior to the addition of PBGT vesicles. Once again, the inhibition of PBGT vesicle binding (both lipid and protein) was sensitive to the protein/lipid molar ratio of the vesicle population, indicating that intact PBGT vesicles were being inhibited from binding. Vesicles with very few PBGT molecules per vesicle, previously able to bind to AchR, were strongly inhibited by αBGT while vesicles with much higher numbers of PBGT molecules per vesicle were only partially inhibited, indicating that some vesicles were apparently stronger binders than the native toxin itself. Furthermore, the inhibition exhibited a strong dependence upon vesicle protein/lipid molar ratio very similar to that seen in the absence of αBGT. The larger difference in percent inhibition of lipid binding vs. percent inhibition of PBGT binding seen at high protein/lipid molar ratios is probably due to a larger heterogeneity in those vesicles that are bound to microsacs in the absence of excess toxin especially when the protein/lipid ratio of the overall vesicle population is high. A similar experiment in which αBGT was first mixed with the PBGT vesicles and then incubated with microsacs showed identical results (data not shown), indicating that true equilibrium competition had occurred during the 5-h incubation of PBGT vesicles with microsacs preincubated with αBGT.

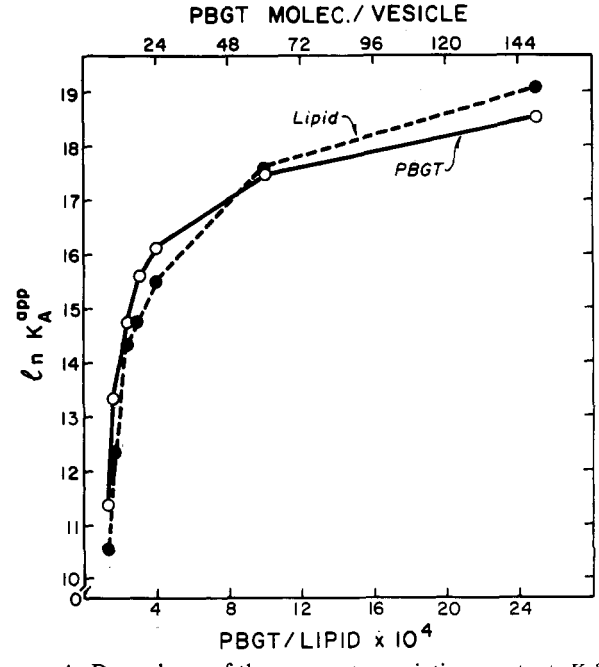

FIGURE 4: Dependence of the apparent association constant, K_A^{app}, for the binding of PBGT vesicles to AchR-enriched microsac membranes upon the PBGT vesicle protein/lipid molar ratio. K_A^{app} values were calculated from the slopes of Scatchard analyses of the binding data.

In order to determine the binding affinity of the PBGT vesicles for microsac membranes, we measured the apparent association constant, K_A^{app}, for the binding as a function of the protein/lipid molar ratio of the vesicles. As shown in Figure 4, the apparent affinity of the vesicles for microsacs was again a sensitive function of the protein/lipid molar ratio, increasing sharply to a maximum of 1.9×10^8 M^{-1} at the highest protein/lipid molar ratio tested. A comparison of the K_A^{app} for vesicle binding to microsacs at the lowest protein/lipid molar ratio (1.3×10^{-4}) at which accurately detectable specific binding occurred vs. the highest ratio tested (2.5×10^{-3}) indicates that there was an apparent 4800-fold increase

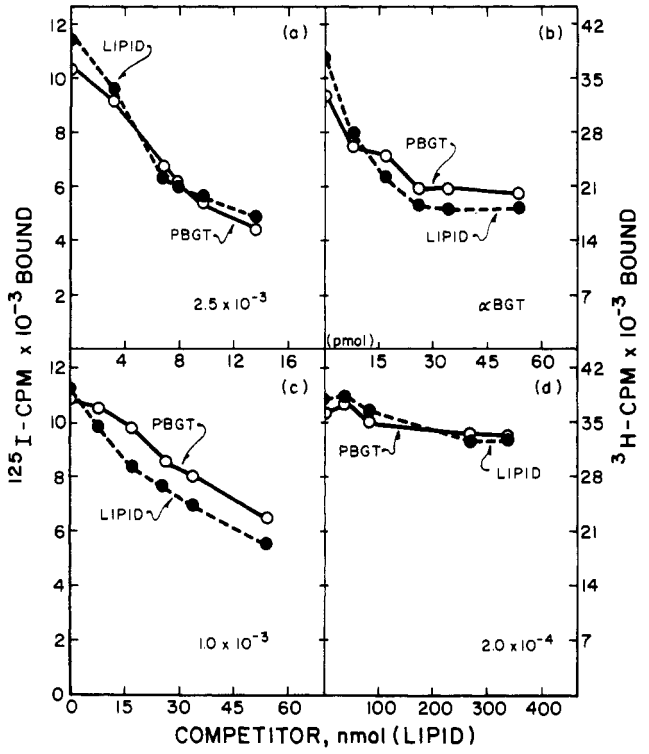

FIGURE 5: Inhibition of radiolabeled PBGT vesicle (protein/lipid molar ratio of 2.5×10^{-3}) binding to AchR-enriched microsac membranes by unlabeled αBGT (b) and PBGT vesicles (a, c, and d) at the indicated protein/lipid molar ratios.

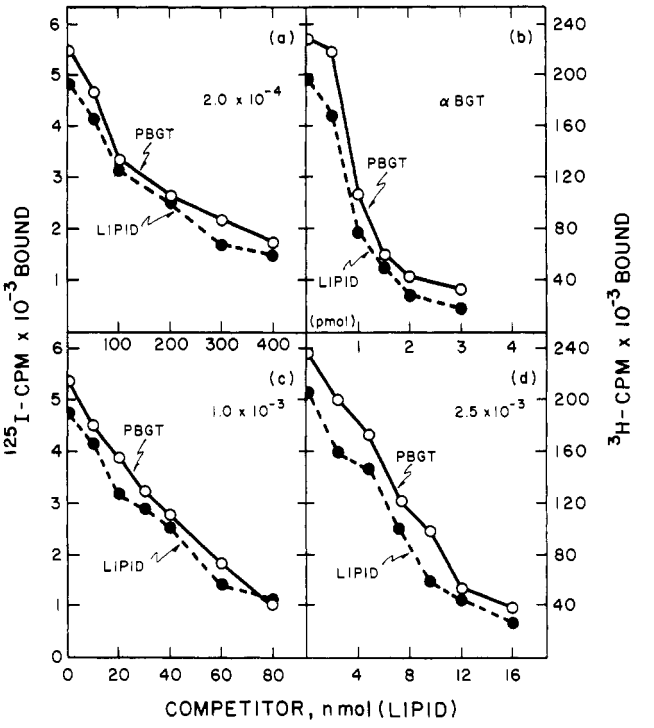

FIGURE 6: Inhibition of radiolabeled PBGT vesicle (protein/lipid molar ratio of 2.0×10^{-4}) binding to AchR-enriched microsac membranes by unlabeled αBGT (b) and PBGT vesicles (a, c, and d) at the indicated protein/lipid molar ratios.

in the lipid vesicle–microsac membrane affinity due to an approximate 20-fold increase in the ligand (PBGT) density on the vesicle surface. Furthermore, the sharp rising portion of the curve occurs at the same approximate number of PBGT per vesicle as was seen in the measurements of percent binding (Figure 2) and percent inhibition of binding with αBGT (Figure 3).

To test the relative binding affinities of the various PBGT vesicle preparations, we measured the direct competition of vesicles at various protein/lipid molar ratios for binding to AchR-enriched microsac membranes under conditions in which the number of binding sites were limited. In Figure 5 are shown the results of an experiment in which 6.80 nmol (17 pmol of vesicle-associated PBGT, just enough to saturate all AchR sites in 2 μg of microsac protein) of radiolabeled PBGT vesicle lipid at a protein/lipid molar ratio of 2.5×10^{-3} (our strongest binder) was separately mixed with increasing amounts of various unlabeled competitors and then assayed for equilibrium binding to the receptor membranes. As shown in the figure, the ability of the various vesicle preparations (competitors) tested to inhibit the binding of the radiolabeled vesicles to microsacs depended strongly upon the protein/lipid molar ratio of the competitor in a manner consistent with all of our previous results. In panel a, it can be seen that it required approximately 8.64 nmol of unlabeled PBGT vesicle lipid at a protein/lipid molar ratio of 2.5×10^{-3} to inhibit 50% of the binding of the radiolabeled vesicles at the same protein/lipid ratio (self-inhibition). As shown in panel b, the use of native αBGT as a competitor in the range of 0–25 pmol was as effective as the unlabeled PBGT vesicles at a protein/lipid molar ratio of 2.5×10^{-3} (self-inhibition) but leveled off in the range of 25–50 pmol perhaps due to an inability to inhibit the stronger binders within the radiolabeled vesicle population. PBGT vesicles at a protein/lipid molar ratio of 1.0×10^{-3} (medium binders, panel c) were able to inhibit 50% of the binding of the radiolabeled vesicles but at a level of competitor approximately 6-fold higher than the amount needed for self-inhibition. Finally, PBGT vesicles at a protein/lipid molar ratio of 2.0×10^{-4} (weak binders, panel d) even when used in a 50-fold excess of the radiolabeled vesicles were only able to inhibit approximately 14% of the binding of the strong binders. As a control, a large excess (68 nmol) of vesicle lipid without any associated PBGT was mixed for 5 h with 6.80 nmol of the radiolabeled vesicle lipid and then shown not to inhibit their binding to microsacs. This result indicated that protein-free lipid vesicles by themselves did not directly inhibit PBGT vesicle binding to AchR-enriched membranes nor indirectly "inhibit" the binding due to transfer of PBGT from the radiolabeled vesicles to the bare vesicles which would effectively decrease the protein/lipid molar ratio with a consequent decrease in binding.

In Figure 6 are shown the results of an experiment in which 215 nmol (43 pmol of vesicle-associated PBGT, just enough to saturate all AchR sites in 8 g of microsac protein) of radiolabeled PBGT vesicle lipid at a protein/lipid molar ratio of 2.0×10^{-4} (a weak binder) was separately mixed with increasing amounts of various unlabeled competitors and then assayed for equilibrium binding to the receptor membranes. As shown in the figure, the ability of the various vesicle populations tested to inhibit the binding of the radiolabeled vesicles to microsacs was once again strongly dependent upon the protein/lipid molar ratio of the competitor. In panel a, it can be seen that it required approximately 186.5 nmol of unlabeled PBGT vesicle lipid at a protein/lipid molar ratio of 2.0×10^{-4} to inhibit 50% of the binding of the radiolabeled vesicles at the same protein/lipid molar ratio (self-inhibition). However, as shown in panel b, only 1 pmol of native αBGT was required for 50% inhibition of the radiolabeled vesicles, indicating that native toxin is a much stronger binder than these vesicles. In panels c and d are shown the effects of addition of unlabeled PBGT vesicles at protein lipid molar ratios of 1.0×10^{-3} and 2.5×10^{-3}, respectively, on the binding

of the radiolabeled vesicles. Approximately 7.85 nmol of PBGT vesicle lipid at a protein/lipid molar ratio of 2.5×10^{-3} (strong binder) and 41.76 nmol of PBGT vesicle lipid at a protein/lipid molar ratio of 1.0×10^{-3} (medium binder) were required to achieve 50% inhibition of the radiolabeled vesicle binding. Therefore, although direct measurement of the apparent association constant, K_A^{app}, for the strong vs. the weak binder had previously indicated an approximate 4800-fold difference in the vesicle binding affinity to AchR-enriched microsacs, the competition results showed only an apparent 24-fold difference in vesicle binding affinity. Although the reason for this discrepancy is not intuitively clear, it can be explained from the standpoint that the relative amount of strong binder vesicle lipid needed for 50% inhibition of a weaker binder depends strongly upon the binding affinity of the weak binder itself. For example, let us assume that 50 radiolabeled weak binders are incubated with microsacs, and at saturation, 12% or six vesicles are bound, leaving 44 vesicles free or unbound. The addition of only 3 unlabeled very strong binders to the incubation mixture should easily displace 3 of the radiolabeled weak binders (50% inhibition) at equilibrium, while, of course, the addition of 50 unlabeled weak binders would be required for the same level of inhibition (self-inhibition). A simple calculation will point out that the amount of strong binder needed for 50% inhibition can be no greater than 17-fold less than the amount of weak binder, regardless of the actual difference in binding affinity of the two vesicle populations. In addition, the replacement of a weak binder on the microsac surface by a much stronger binder necessarily brings more vesicle-associated PBGT along with the vesicle lipid than was previously present on the displaced weaker binders, leading once again to an underestimate of the difference in relative binding affinities of the vesicle-associated PBGT. Finally, the absolute amount of competitor required for 50% inhibition is strongly dependent upon the experimental conditions, especially the degree of saturation of the total available AchR sites occupied by the radiolabeled weak binder. We chose to measure competition between the various vesicle populations for binding to AchR-enriched microsacs when sites are limited in order to guarantee that whenever a competitor vesicle bound to the microsacs a weaker binding vesicle was necessarily replaced.

Thermodynamic Analysis of the Temperature Dependence of Binding. In Figure 7 are shown the results of an experiment in which αBGT and PBGT binding affinity for Triton X-100 solubilized AchR was measured as a function of temperature. Also shown in the figure is the temperature dependence of the binding affinity of a weak (protein/lipid molar ratio = 1.3×10^{-4}), medium (protein/lipid molar ratio = 3.0×10^{-4}), and strong (protein/lipid molar ratio = 2.5×10^{-3}) PBGT vesicle binder to AchR-enriched microsac membranes. The apparent association constant, K_A^{app}, for both PBGT and αBGT binding to detergent-solubilized AchR as well as for PBGT vesicle binding to microsac membranes increased with increasing temperature. As shown in Table I, the binding of both αBGT and PBGT to detergent-solubilized AchR is entropically driven $\Delta S°$(BGT–AchR) = 58.2 eu (cal deg^{-1} mol^{-1}) and $\Delta S°$-(PBGT–AchR) = 66.9 eu; i.e., since the binding of αBGT and PBGT to AchR results in an overall increase of enthalpy [$\Delta H°$(αBGT–AchR) = 6.3 kcal/mol and $\Delta H°$(PBGT–AchR) = 10.7 kcal/mol], it is only because of the relatively large increase in entropy upon binding that the binding reaction itself is exergonic. The binding of all three vesicle preparations to AchR microsacs was also endothermic and therefore entropically driven (Table I), indicating that the interaction of vesicles

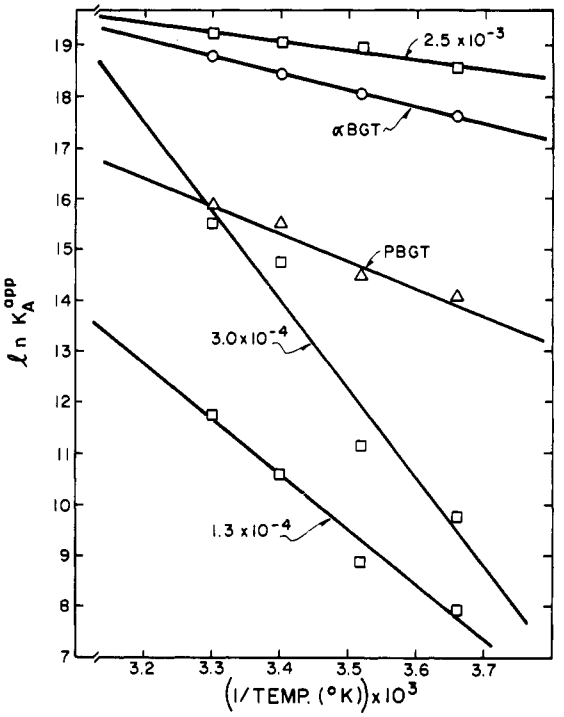

FIGURE 7: van't Hoff plots of the temperature dependence of the apparent association constant, K_A^{app}, for the binding of αBGT (○) and PBGT (△) to detergent-solubilized AchR and PBGT vesicles (□) at the indicated protein/lipid molar ratios to AchR-enriched microsac membranes. Straight lines are least-squares fits of the data with correlation coefficients greater than 0.94.

Table I: Thermodynamic Parameters for Binding of αBGT and PBGT to Detergent-Solubilized AchR and PBGT Vesicles to AchR-Enriched Microsac Membranes

ligand	$\Delta G°_{298}$ (kcal/mol)[a]	$\Delta H°$ (kcal/mol)[b]	$\Delta S°$ (eu[c])[b]
αBGT[d]	−10.8	6.3	58.2
PBGT	−9.1	10.7	66.9
PBGT vesicle[e]			
1.3×10^{-4}[f]	−6.3	12.7	63.8
3.0×10^{-4}[f]	−8.8	27.2	120.6
2.5×10^{-3}[f]	−11.3	3.3	49.0

[a] Standard Gibbs free energy change calculated from the equation $\Delta G° = -RT \ln K_A^{app}$. [b] Enthalpy ($\Delta H°$) and entropy ($\Delta S°$) changes calculated from the integrated van't Hoff equation $\ln K_A^{app} = -\Delta H°/RT + \Delta S°/R$. [c] Entropy units (cal deg^{-1} mol^{-1}). [d] Binding to detergent-solubilized AchR. [e] Binding to AchR-enriched microsac membranes. [f] Protein/lipid molar ratio.

with microsacs was probably mediated by the interaction of PBGT with the AchR. The binding of PBGT vesicles at a protein/lipid molar ratio of 1.3×10^{-4} (weak binder) resulted in a positive reaction enthalpy ($\Delta H°$ = 12.7 kcal/mol of lipid) and a positive reaction entropy ($\Delta S°$ = 63.8 eu) values which were similar to those for the PBGT–AchR interaction in detergent. The binding of PBGT vesicles at a protein/lipid molar ratio of 3.0×10^{-4} (medium binder) exhibited a larger positive reaction enthalpy ($\Delta H°$ = 27.2 kcal/mol of lipid) and a larger positive reaction entropy ($\Delta S°$ = 120.6 eu), values which may indicate that the difference between the binding affinity of the weak vs. the medium strength PBGT vesicle binder for AchR-enriched microsacs is simply due to an increase in the total number of PBGT–AchR bridges (mediating the binding between vesicles and microsacs) that contribute to the overall binding reaction enthalpy and entropy in an approximately additive fashion. The thermodynamic parameters for the interaction of our strongest PBGT vesicle binder (protein/lipid molar ratio of 2.5×10^{-3}) with AchR-enriched microsacs ($\Delta H°$

= 3.3 kcal/mol of lipid and ΔS° = 49.0 eu) indicate that a further increase in the number of PBGT–AchR bridges contributing in an additive manner to the overall reaction enthalpy and entropy does not apply in the interaction of these strong binders with microsac membranes. The ΔH° for this vesicle population binding to AchR-enriched membranes was approximately 8-fold lower than that for the medium binder, indicating that some additional favorable binding energy was present only in the interaction of these strong binders with microsacs. It was also surprising that the entropy of the binding reaction decreased to a value approximately 41% of that seen with binding of PBGT vesicles at a protein/lipid molar ratio of 3×10^{-4} (medium binder).

Discussion

Although the implications of monovalent and multivalent interactions (from the standpoint of antigen–antibody binding) have been discussed by Karush (1978), who defined intrinsic affinity as the parameter of monovalent interaction and functional affinity as the parameter of multivalent interaction, the derivation of functional affinity from intrinsic affinity based upon theoretical principles is difficult mainly because it depends upon the number, spatial arrangement, and motional freedom of antibody and antigen binding sites. However, it has been possible in a few cases to measure functional affinity empirically; for example, Hornick & Karush (1969) have determined a special type of functional affinity by measuring by equilibrium dialysis the inactivation of dinitrophenolated bacteriophage T_4 with anti-dinitrophenol antibodies and showing that the functional affinity of anti-dinitrophenol IgG was between 2×10^4 and 6×10^4 times greater than its intrinsic affinity. This difference presumably arose from the multivalency of the antibody and, in particular, to a lower dissociation rate constant for the antibody, with the association rate constant being unchanged. In addition, Hornick & Karush (1972) have further shown that the functional affinity of anti-dinitrophenol IgM is much higher than that of anti-dinitrophenol IgG, with a comparable intrinsic affinity for the monovalent antigen (dinitrophenol–lysine); therefore, an antibody with 10 binding sites bound to a multivalent antigen with greater affinity than an antibody with 2 binding sites of similar intrinsic affinity. Recently, Heath et al. (1984) have extended these results by measuring the binding affinity of vesicles conjugated with antifluorescein antibody for fluorescein isothiocyanate modified erythrocytes and found that the functional affinity of vesicles for modified red blood cells (RBCs) was up to 1000-fold greater than the intrinsic affinity of the antibody for soluble ligand.

We have developed a simple, well-defined, and highly flexible model system with which to systematically study specific membrane interactions. This system does not suffer from the added complications due to receptor–ligand metabolism, membrane complexity, unknown secreted factors, cellular heterogeneity, etc. present in other cell–cell recognition systems. We are able to prepare vesicles at a very wide range of ligand (PBGT) densities that are homogeneous in size with the added advantage that all ligands are exposed on the surface. The location of the acyl chain in the PBGT molecule has been identified as Lys_{51} (Babbitt & Huang, 1985) so that insertion of this chemically homogeneous toxin derivative into the outer leaflet of a lipid vesicle results in a physically homogeneous interaction with the phospholipids. The motional dynamics of this membrane-bound ligand (PBGT) on the vesicle surface as well as its physical interaction with the vesicle bilayer have been extensively characterized (Babbitt et al., 1984). The acylated toxin in fluid bilayers exhibits high lateral and rotational mobility on the surface of a phospholipid vesicle. In addition, the motional and binding characteristics of the AchR in microsac membrane vesicles have been extensively studied (Rousselet & Devaux, 1977; Axelrod et al., 1976), as well as the biochemical and biophysical parameters of the αBGT–AchR interaction itself. Finally, the binding of our PBGT vesicles to AchR-enriched microsacs inhibits the ion channel activity of the microsacs, strongly indicating that the binding interaction is mediated by specific interactions with AchRs (Grant et al., 1982). Therefore, we feel that our system best lends itself to a rigorous analysis of the type necessary to explore some physicochemical characteristics of membrane interactions mediated by specific receptor–ligand binding.

The first important conclusion drawn from the various binding results presented in this paper is that the multivalent nature of the vesicle-associated PBGT is a critical determinant of the strength of binding of PBGT vesicles to AchR-enriched microsac membranes. We have observed a dramatic increase in the apparent equilibrium binding affinity of PBGT vesicles (approximately 4800-fold) for AchR-enriched microsacs as the protein/lipid molar ratio of the vesicles was increased approximately 20-fold (Figure 4). When compared to vesicles without associated PBGT which do not bind with microsacs, this enhancement is quite impressive. This result is presumably due to an increase in the actual number of AchR–PBGT bridges mediating the binding of the lipid vesicles to the microsacs. Our observation is in agreement with that seen with antibody–antigen binding in which the apparent functional affinity of a bivalent molecule (e.g., IgG) is about 1–2 orders of magnitude higher than that of the intrinsic affinity of the corresponding monovalent molecule (e.g., Fab) (Karush, 1976). Another interesting aspect of these results is the existence of a threshold level of PBGT vesicle protein/lipid molar ratio at which there occurs a large increase in the specific binding of the vesicles to microsacs. Since the AchR density on the microsac surface is quite high, about 10^4 receptors/μm^2 (Heuser & Saltpeter, 1979), and since vesicle-associated PBGT has a high degree of lateral mobility [allowing diffusion into close proximity to the receptor, perhaps forming a contact cap (Bell, 1979)] and also a high degree of rotational mobility (to achieve proper orientation for stereospecific binding with AchR once close contact occurs), it is not surprising that the threshold level of PBGT per vesicle required to achieve strong binding is quite low, namely, six per vesicle. Bell et al. (1984) predict the existence of such a "phase transition" (threshold phenomenon) marking the onset of stable cell–cell or cell–substratum adhesion which results from the competition between attractive forces resulting from the formation of specific macromolecular bridges, and nonspecific repulsion arising from electrostatic forces and osmotic forces, mostly associated with the glycocalyx (these repulsive forces should be minimal in our system). Solid experimental evidence confirming the existence of such a critical point has not been easy to find although threshold phenomena have previously been reported in a few systems (Weigel et al., 1979; Huang, 1985). Since all vesicle-associated PBGT in our system is exposed on the surface of the vesicle and since there are approximately 60 000 phospholipid molecules per 800-Å vesicle (Enoch & Strittmatter, 1979), we can calculate that the surface density of PBGT on the vesicle at the threshold binding level is approximately 2.98×10^2 molecules/μm^2 which is approximately 34-fold lower than the AchR surface density. As mentioned previously, since the AchR itself is essentially immobile, it appears that a highly mobile ligand (PBGT) can bind efficiently to a relatively immobile receptor (AchR).

Another interesting aspect of our results is the shape of the curve of ln K_A^{app} vs. PBGT vesicle protein/lipid molar ratio (Figure 4). To our knowledge, this is the first published data of its kind. At protein/lipid molar ratios between 1.3×10^{-4} and 4.0×10^{-4}, there is a sharp increase in the ln K_A^{app}, presumably due to an increase in the number of PBGT–AchR bridges mediating the binding of the lipid vesicles to the microsac membranes. This phenomenon has been predicted by Bell et al. (submitted for publication) and referred to as the phase of cell–cell adhesion in which the onset of maximum cell–cell contact occurs. At protein/lipid molar ratios greater than 4.0×10^{-4}, there is an apparent decrease in the effect of increasing PBGT density on the vesicle surface upon lipid vesicle–microsac membrane binding affinity. This result may reflect the onset of saturation in the total number of PBGT–AchR bonds able to be formed between the vesicles and microsacs (under conditions of maximum vesicle–microsac contact area). It is interesting to note that at the onset of this portion of the curve the calculated density of the ligand (PBGT) on the vesicle surface is approaching that of the AchR density on the microsac. Perhaps the levelling off of the dependence of ln K_A^{app} upon PBGT vesicle protein/lipid molar ratio results from a saturation of available AchRs present in the contact region, upon interaction of microsacs with vesicles containing PBGT at an equal density; all that is required of the PBGT ligands is that they be able to freely rotate, allowing stereospecific binding to the immobile AchRs. Once all of the AchRs present in the contact area are involved in receptor–toxin complexes, further increases in the density of PBGT on the vesicle surface should have little effect on the vesicle–microsac binding affinity, so that a maximum in the ln K_A^{app} vs. PBGT/lipid molar ratio curve is reached. Another potentially important factor in the determination of the dependence of ln K_A^{app} upon PBGT density is the contact area between the vesicles and microsacs. Even when the densities of PBGT and AchR are the same, the total number of bridges formed between the lipid vesicles and the microsac membranes should be strongly dependent upon the contact area; the greater the contact area, the greater the number of receptor–toxin bridges mediating the binding, and consequently the greater the K_A^{app}. Therefore, another plausible explanation for the leveling off of the curve is that excess PBGT molecules present on bound (to microsacs) vesicle surfaces cannot approach AchRs closely enough to form true receptor–toxin complexes due to geometric or curvature constraints in the microsacs and/or the lipid vesicles. This can happen even though noncomplexed receptors and highly mobile [even at the highest protein/lipid molar ratios (2.5×10^{-3}) used] PBGT are present in their respective membranes and available for binding. Of course, it is possible that other mechanisms such as packing problems in the microsac–vesicle contact area, negative cooperativity in the binding, and perturbation of the membrane(s) itself, to name a few, occurring once a saturation number of PBGT–AchR bridges have formed, could explain these data.

Data from the competition experiments shown in Figures 5 and 6 indicated that increasing the protein/lipid molar ratio of the PBGT vesicles increased the ability of the vesicle preparation to compete for binding to limited sites on AchR-enriched microsacs. The competition data agree qualitatively with the data from direct binding experiments, and quantitative differences due to the experimental conditions were fully addressed under Results. Nevertheless, the significance of these results lies in the fact that a multivalent binder is a stronger binder and can easily replace binders of lower valency and even monovalent binders of the same intrinsic affinity. Perhaps the variation of valency is an important regulatory mechanism in determining the specificity of cell–cell or cell–substratum binding in vivo, in which case sites are often limited so that recognition actually proceeds under conditions of competition.

The temperature dependence of the apparent association constant, K_A^{app}, for the binding of αBGT and PBGT to detergent-solubilized AchR indicated that the binding reaction was endothermic and exergonic since the highly positive reaction entropies (Table I) more than compensated for the positive reaction enthalpies. The magnitudes of the αBGT, PBGT–AchR binding reaction entropies are surprisingly large, since ΔS° values for most chemical reactions or protein binding reactions, where information transfer is not involved, fall in the range of +20 to −30 eu. Furthermore, van't Hoff plots of the binding data (Figure 7) were linear over the temperature range studied, indicating that both the enthalpy change and the entropy change for the overall binding reaction were independent of temperature. This result argues against the binding of αBGT and PBGT to AchR being due largely to hydrophobic effects (Edelhock & Osborne, 1976). Therefore, the data imply substantial structural rearrangements accompanying the αBGT, PBGT–AchR binding interaction, most presumably due to a ligand-induced receptor conformational change. Maelicke et al. (1977) reached a similar conclusion upon finding that a comparably large positive reaction entropy accompanied the binding of both small and large agonists and antagonists (including α-cobratoxin) to detergent-solubilized AchRs, thereby driving the binding of various ligands to the receptor accompanied by large positive reaction enthalpies. The higher positive reaction enthalpy accompanying PBGT binding to AchR compared to αBGT binding to AchR may be due to the loss of an interaction of the ϵ-amino group of Lys_{52} with the receptor. This residue is presumably no longer able to directly interact with AchR when the toxin is attached to the surface of a lipid vesicle upon insertion via the acyl chain which is covalently bound to the ϵ-amino group of Lys_{51} of the PBGT molecule (Babbitt & Huang, 1985).

The temperature dependence of the apparent association constant, K_A^{app}, for the binding of PBGT vesicles to AchR-enriched microsacs indicated that the binding, similar to the case of the αBGT, PBGT–AchR interaction, was once again endothermic and therefore entropically driven. To our knowledge, this is the first report of the thermodynamic parameters for the binding of two membranes mediated by specific ligand–receptor binding. PBGT vesicles at protein/lipid molar ratios of 1.3×10^{-4} and 3.0×10^{-4} appeared to bind in a similar fashion as monovalent PBGT to AchR, since the ΔH° and ΔS° values for reaction of each of these two vesicle preparations with AchR-enriched microsac membranes increased in an additive fashion presumably due to an increase in the number of receptor–toxin bonds mediating the interaction of the two membranes. However, the large decrease in both ΔH° and ΔS° values accompanying interaction of vesicles at a protein/lipid molar ratio of 2.5×10^{-3} with microsacs indicates the presence of some additional exothermic interaction(s) (or a completely different type of interaction altogether) between these strong binders and the microsac membranes. The explanation for these data at this point in time is not known. However, it is interesting to note that in their thermodynamic modeling of cell adhesion Bell et al. (1984) predict that at high ligand–receptor densities, following a phase of increasing cell–cell contact area mediated by increasing numbers of receptor–ligand bridges (perhaps the sharp rising portion of the curve in Figure 3), there will occur a

decrease in the contact area to a value approximately 50% of the maximal value ("rounding up" of the cell). If the receptor–ligand density is sufficiently large, then all available receptors and ligands can be saturated without the need for maximum contact. Consequently, the driving force for spreading is decreased and the cell starts to round up under the influence of the nonspecific repulsive forces. Perhaps in our system the difference in $\Delta H°$ and $\Delta S°$ values for our strongest PBGT vesicle binder vs. the weak and medium strength PBGT vesicle binders reflects a difference in vesicle–microsac contact area.

The results described in this paper concerning the effects of valency on the thermodynamics of specific membrane interactions should allow a more rigorous analysis of the validity of explicit predictions concerning cell adhesion derived from theoretical works.

The recent theoretical models proposed by Bell et al. (1984) and by Dembo & Bell (1985) have made some explicit predictions concerning the thermodynamics of cell–cell adhesion. We have attempted to use their theory with measured or reasonably estimated parameters to fit our experimental results. We were successful in using the theory to describe threshold binding phenomenon. However, under no circumstances were we able to fit the data in Figure 2 with their equations. This suggests to us that a more refined theoretical model is needed to describe our model system. We are currently pursuing this route.

REFERENCES

Axelrod, D., Raudin, P., Koppel, D. E., Schlessinger, J., Webb, W. W., Elson, E. L., & Podleski, T. R. (1976) *Proc. Natl. Acad. Sci. U.S.A. 73*, 4594–4598.

Babbitt, B. P., & Huang, L. (1985) *Biochemistry 24*, 15–21.

Babbitt, B. P., Huang, L., & Freire, E. (1984) *Biochemistry 23*, 3920–3926.

Bell, G. I. (1979) in *Physical Chemical Aspects of Cell Surface Events in Cellular Regulation* (DeLisi, C., & Blumenthal, R., Eds.) Elsevier/North-Holland, New York.

Bell, G. I., Dembo, M., & Bongrand, P. (1984) *Biophys. J.* (submitted for publication).

Chen, Y. H., Tai, J. C., Huang, W. J., Lai, M. Z., Hung, M. C., Lai, M. D., & Yand, T. T. (1982) *Biochemistry 21*, 2592–2500.

Dembo, M., & Bell, G. I. (1985) *Curr. Top. Membr. Transp.* (in press).

Edelhoch, H., & Osborne, J. C., Jr. (1976) *Adv. Protein Chem. 30*, 183–250.

Edelman, G. M. (1983) *Science (Washington, D.C.) 219*, 450–457.

Enoch, H. G., & Strittmatter, P. (1979) *Proc. Natl. Acad. Sci. U.S.A. 76*, 145–149.

Frazier, W., & Glaser, L. (1979) *Annu. Rev. Biochem. 48*, 491–523.

Frazier, W. A., Glaser, L., & Gottlieb, D. I., Eds. (1982) in *Cellular Recognition*, Alan R. Liss, New York.

Grant, S. W., Babbitt, B. P., West, L. K., & Huang, L. (1982) *Biochemistry 21*, 1274–1279.

Heath, T. D., Fraley, R. T., Bentz, J., Voss, E. W., Herron, J. N., & Papahadjopoulos, D. (1984) *Biochim. Biophys. Acta 770*, 148–158.

Heuser, J. E., & Salpeter, S. R. (1979) *J. Cell Biol. 82*, 150–173.

Hornick, C. L., & Karush, F. (1969) *Isr. J. Med. Sci. 5*, 163–170.

Hornick, C. L., & Karush, F. (1972) *Immunochemistry 9*, 325–340.

Huang, L. (1985) *Biochemistry 24*, 29–34.

Karush, F. (1976) *Contemp. Top. Mol. Immunol. 5*, 217–228.

Karush, F. (1978) *Compr. Immunol. 5*, 85–116.

Maelicke, A., Fulpius, B. W., Klett, R. P., & Reich, E. (1977) *J. Biol. Chem. 252*, 4811–4830.

Pool, G. L., French, M. E., Edwards, R. A., Huang, L., & Lumb, R. H. (1982) *Lipids 17*, 448–452.

Rousselet, A., & Devaux, P. F. (1977) *Biochem. Biophys. Res. Commun. 78*, 448–454.

Ruter, W. J. (1978) *Symp. Soc. Dev. Biol. 35*, 3–10.

Scatchard, G. (1949) *Ann. N.Y. Acad. Sci. 51*, 660–672.

Springer, W. R., & Barondes, W. R. (1982) *Proc. Natl. Acad. Sci. U.S.A. 79*, 6561–6565.

Subtelny, S., & Wessels, N. K., Eds. (1980) in *The Cell Surface: Mediator of Developmental Processes*, Academic Press, New York.

Weigel, P. H., Schnaar, R. L., Kahlenschmidt, M. S., Schmell, E., Lee, R. T., Lee, Y. C., & Roseman, S. (1979) *J. Biol. Chem. 254*, 10830–10838.